Characteristics of Turbulence Driven Multiple-Channel Transport in Tokamaks, and Comparison with Experiments

W. X. Wang, T. S. Hahm, S. Ethier, G. Rewoldt, S. M. Kaye, W. M. Tang, W. W. Lee

Princeton Plasma Physics Laboratory, P. O. Box 451, Princeton, New Jersey 08543, USA

P. H. Diamond

University of California, San Diego, California 92093, USA

wwang@pppl.gov

Abstract. Recent progress made with our global gyrokinetic simulations in understanding the origin of intrinsic rotation and non-diffusive transport characteristics in tokamaks is reported. Key results include the finding of an important nonlinear flow generation process due to the residual stress produced by the fluctuation intensity and the intensity gradient, acting with the zonal flow shear induced $k_\parallel$ symmetry breaking, which offers a universal mechanism to drive intrinsic rotation via wave-particle momentum exchange. This turbulence nonlinearly-driven intrinsic rotation scales close to linearly with plasma gradients and the inverse of the plasma current in various turbulence regimes, reproducing and extending empirical scalings obtained in multiple fusion devices. The underlying physics governing these characteristic dependences is elucidated. Particularly, the current scaling is found to result from the magnetic shear effect on $k_\parallel$ symmetry breaking. Highlighted results also include robust radial pinches in toroidal flow, heat and particles driven by CTEM turbulence, which emerge "in phase", and are shown to play remarkable roles in determining plasma transport. Particularly, the "flow pinch" phenomenon amazingly reproduces the experimental result of radially inward penetration of perturbed flows created by modulated beams in peripheral regions, and thus is highly illuminating. Finally, the ∇T_e-driven CTEM turbulence in specific parameter regimes is found to generate remarkably large fluctuation structures via inverse energy cascades, which may have a natural connection to the generation of blobs in the edge.'

I. Introduction

Momentum transport and plasma flow generation are complex transport phenomena of great importance in magnetic confinement fusion. An optimized plasma flow is believed to play a critical role in both controlling macroscopic plasma stability, and in reducing energy loss due to plasma microturbulence. On the other hand, toroidal momentum transport is observed to be highly anomalous, non-diffusive and non-local in nearly all machines. A striking phenomenon found in experiments is the intrinsic or spontaneous rotation; namely, toroidal plasmas can self-organize and develop rotation without an external torque [1]. In fact, the intrinsic rotation in fusion plasmas is an example of a "negative viscosity phenomenon" in which an up-gradient component of the momentum flux organizes a structured mean flow. Negative viscosity phenomena are of broad interest in the context of atmospheres, oceans, stellar interiors, and other rotating fluids. In current fusion experiments, a large plasma rotation can be driven by neutral beam injection which also provides momentum input while heating the plasma. In large size burning plasmas, however, the use of neutral beams for plasma heating becomes very challenging. It is expected that intrinsic rotation will dominate in future burning plasma experiments. Therefore, understanding the non-diffusive momentum transport mechanisms and the intrinsic rotation phenomenon is a key to predicting plasma flow in ITER.

Recently, extensive experimental studies have been carried out on this topic. The parametric dependence of the intrinsic rotation has been statistically characterized using a broad range of experimental data bases obtained in multiple machines. Specifically, the increment of central

intrinsic rotation is shown to increase with the increment of plasma stored energy and to scale with the inverse of the plasma current [2] (the so called Rice scaling). Similar empirical scaling is also observed in other devices including JT-60U [3] and LHD [4], where the intrinsic rotation velocity is shown to increase with the ion pressure gradient in core plasma with an internal transport barrier. There is no doubt that these results are important for making a qualitative projection of plasma rotation in ITER. A more fundamental, critical issue is to understand the underlying physical origins of the experimental empirical scalings. This is the major focus of this study.

In this work, turbulence-driven non-diffusive momentum transport is investigated using the global Gyrokinetic Tokamak Simulation (GTS) code [5] with emphasis on the characteristic dependence of turbulence driven intrinsic rotation on plasma parameters. The GTS code is based on a generalized gyrokinetic simulation model using a δf particle-in-cell approach, and incorporates the comprehensive influence of non-circular cross section, realistic plasma profiles, plasma rotation, neoclassical (equilibrium) electric field, Coulomb collisions, and other features. It can directly read plasma profiles of temperature, density and toroidal angular velocity from the TRANSP experimental database, and a numerical magnetohydrodynamic (MHD) equilibrium reconstructed by MHD codes using TRANSP radial profiles of the total pressure and the parallel current (or safety factor), along with the plasma boundary shape.

Our focus is on the electron transport dominant regime. To simulate electron turbulence and ion turbulence with non-adiabatic electron physics, fully-kinetic electron physics is included in the GTS code [6]. One highlighted feature, distinct from many other gyrokinetic simulations, is that both trapped and untrapped electrons are included in the non-adiabatic response.

II. Nonlinear flow generation by electrostatic turbulence

Out of various possibilities of physical dynamics which may play roles in determining toroidal rotation, the strong coupling between toroidal momentum and energy transport generally observed in fusion experiments [7] suggests that micro-turbulence is a key player. For turbulence driven toroidal momentum flux, a generic structure can be expressed as follows:

$$\Gamma_\phi \propto -\chi_\phi \frac{\partial U_\phi}{\partial r} + V_p U_\phi + \Pi_{r,\phi}^{\mathrm{rs}}.$$

In addition to diffusion (first term), there are two nondiffusive components, momentum pinch (second term) and residual stress (third term). The three components in the momentum flux are highly distinct not only formally but also physically. Besides their different physical origins under turbulence circumstances, they have qualitatively distinct effects on the toroidal flow formation. Note that all three components have been observed in tokamak experiments.

The residual stress $\Pi_{r,\phi}^{\mathrm{rs}}$, which is defined as a specific part of the Reynolds stress with no direct dependence on either the rotation velocity or its gradient, can be shown in the momentum transport equation to be isomorphic in mathematical form to the integrated external momentum source which acts as a torque to drive the rotation. Thus, the residual stress can act as an internal local torque to spin up a plasma, offering an ideal mechanism to drive intrinsic rotation under appropriate boundary conditions. For this reason, the quantity $\nabla \cdot \mathbf{\Pi}_{r,\phi}^{\mathrm{rs}}$ is widely referred to as the intrinsic torque in experimental and theoretical investigations. In a broad physical context, this is a type of wave-driven flow phenomenon which operates via wave-particle momentum exchange [8].

Our global gyrokinetic simulations using the GTS code have revealed an important nonlinear flow generation process due to the residual stress produced by electrostatic turbulence of ion temperature gradient (ITG) modes and trapped electron modes (TEM) [6, 9]. Particularly, in collisionless TEM (CTEM) turbulence, both turbulence fluctuation intensity and the intensity gradient are identified as nonlinear mechanisms for driving residual stress. The latter is associated with the turbulence wave radiation induced wave momentum diffusion. Another key

ingredient for turbulence driven residual stress is symmetry breaking in the parallel wave number spectrum. Such a well know mechanism is the mean $\mathbf{E} \times \mathbf{B}$ flow shear [10, 11]. For most drift wave instabilities, both signs of $k_\parallel$ are equally excited in the ideal case, resulting in a reflection symmetry in the $k_\parallel$ spectrum. Perfect local $k_\parallel$ symmetry means perfectly balanced population density between co- and counter-propagating acoustic waves along the torus, and thus a vanishing net local momentum torque. Therefore, a critical, generic piece of physics behind the residual stress spinning up the plasma is the breaking of the $k_\parallel \to -k_\parallel$ symmetry. Concerning the origin of the symmetry breaking, turbulence self-generated low frequency zonal flow shear has been identified to be a key, universal mechanism in various turbulence regimes. Simulations also indicate the existence of other mechanisms beyond $\mathbf{E} \times \mathbf{B}$ shear.

III. Characteristics of turbulence-nonlinearly-driven plasma flow and origin of empirical scalings of intrinsic rotation

The turbulence-nonlinearly-driven residual stress, acting as an intrinsic torque, is shown to spin up toroidal rotation effectively. In our previous study, ITG turbulence driven "intrinsic" torque is shown to increase close to linearly with plasma pressure gradient [6], in qualitative agreement with experimental observations in various devices. For typical plasma parameters of fusion experiments, collisionless TEM turbulence can be a major source to drive multiple-channel transport, including toroidal momentum transport. However, the momentum transport and flow generation phenomena have not been well explored experimentally in the electron transport dominated regimes. Quantifying the characteristic dependence of turbulence generated toroidal flow in the electron turbulence regimes is particularly important for ITER experiments in which the electron channel is expected to dominate plasma transport.

The characteristic dependence of intrinsic torque driven by CTEM turbulence is numerically investigated. The GTS simulations are carried out over a wide range of experimentally relevant plasma parameters, which cover various regimes with respect to different sources of free energy for driving CTEM turbulence.

First, we examine the dependence of intrinsic rotation on electron pressure gradient. For this parametric scan study, radial profiles of electron density/temperature/pressure gradient used in simulations are specified according to the expression: $R_0/L_{n_e,T_e,p_e} = -\kappa \exp\left[-\left(\dfrac{\rho - \rho_c}{0.28}\right)^6\right]$, along with a fixed density/temperature/pressure at the center $\rho_c = 0.5$. This gives a fairly uniform CTEM drive in a region centered at ρ_c and near zero gradient elsewhere. The simulation scan is performed by varying the κ value. For all these simulations, plasmas are initially rotation-free and momentum-source-free, which allows us to concentrate on the residual stress associated intrinsic torque. An equilibrium $\mathbf{E} \times \mathbf{B}$ shear is also included via the radial force balance relation, which, however, is seen to be a minor player with respect to CTEM self-generated zonal flows. The numerical MHD equilibrium used in this study corresponds to a real DIII-D discharge. All simulations in this paper use 100 particle/cell·species.

Instead of calculating the local torque $\nabla \cdot \mathbf{\Pi}_{r,\phi}^{\mathrm{RS}}$, we examine the rate of toroidal momentum generation, dP_ϕ/dt, associated with the residual stress, with $P_\phi \equiv \int d^3r |\int d^3v m_i R v_\phi \delta f_i|$. Apparently, the quantity dP_ϕ/dt is a measure of the volume-integrated (or spatially averaged) torque driven by turbulence, which has better correspondence to the intrinsic torque inferred from experiments or measured central intrinsic rotation. The simulation results of total intrinsic torque dP_ϕ/dt driven by CTEM turbulence, versus the electron pressure gradient ∇p_e, are summarized in Fig. 1. The three curves in Fig. 1 correspond to three cases of free energy for driving CTEM. The dominant free energy sources are ∇n (black), ∇T_e (green) and a combination of both (red), respectively. For all three cases, the intrinsic torque associated with nonlinearly generated residual stress is found to increase close to linearly with the electron pressure gradient. In the other words, a larger central intrinsic rotation is expected to be produced in a plasma with a higher elec-

tron pressure gradient. The dominant underlying physics governing this scaling is rather straightforward, namely, both the turbulence intensity and the zonal flow shear, which are two key ingredients for driving residual stress, are increased with the strength of the CTEM drive R_0/L_{p_e}.

Moreover, the observation of the black curve being above the green and red curves indicates that the free energy in the density gradient is more efficient in driving intrinsic rotation via CTEM turbulence. These results predicted from the gyrokinetic simulations suggest a strong connection between intrinsic rotation and electron parameters. It is highly interesting to test this prediction in experiments. As a good opportunity for validation study, particularly, NSTX experiments can be used as a unique platform to test the predicted characteristic dependence of intrinsic rotation on electron parameters in electron transport dominated regimes.

Figure 1: CTEM-driven total intrinsic torque (spatially averaged) versus electron pressure gradient R_0/L_{p_e}.

Now we turn to exploring the dependence of residual stress and intrinsic rotation on the plasma current I_p. Again, this simulation study is carried out for CTEM turbulence. The primary purpose is to attempt to shed light on the physics origin of the current scaling which was obtained in multiple devices [2]. For this simulation study we adopt a similar methodology to that used in experiments for various investigations of current scans. A set of simulation experiments is carried out by holding the vacuum (external) magnetic field and plasma pressure profile fixed, while varying the plasma current. Specifically, this is accomplished by generating a series of shaped, numerical equilibria with $I_p = 0.75$, 1.0, 1.5 and 2.0 MA, using an MHD code.

The major parameters used in this study are: $R_0/L_{T_e} = R_0/L_n = 6$, $R_0/L_{T_i} = 2.4$ and 100 particles/cell·species. Simulation results presented in the right panel of Fig. 2 show that the rate of toroidal momentum generation by CTEM turbulence (i.e, total intrinsic torque) increases close to linearly with the inverse of the plasma current. This result indeed reproduces the same trend as that of the Rice scaling. With respect to the torque versus ∇T, ∇n and ∇p scaling in the ITG and CTEM turbulence, however, the underlying physics governing the current scaling is less transparent.
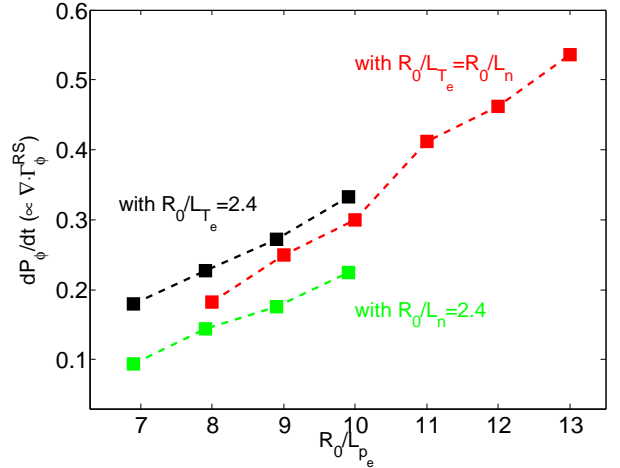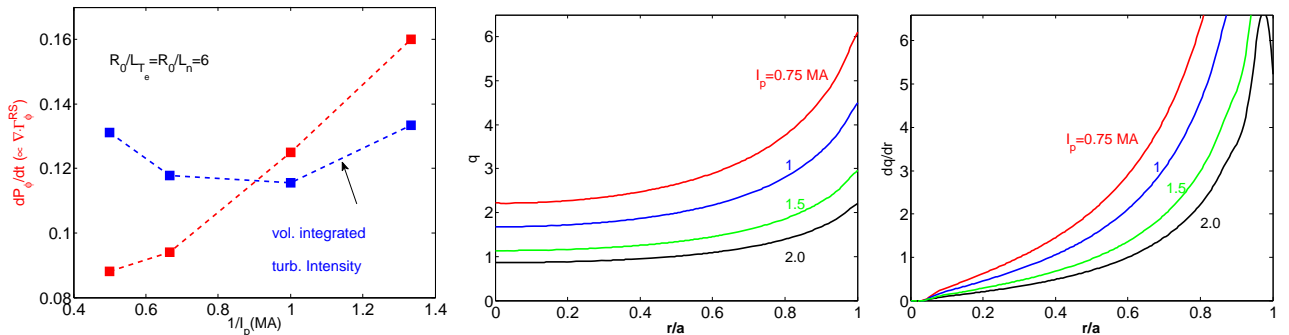

Figure 2: CTEM-driven total intrinsic torque and volume-integrated turbulence intensity at steady state versus plasma current I_p (left), and corresponding radial profiles of safety factor q (middle) and magnetic shear dr/dr (right) of the four cases.

Both turbulence intensities and intensity gradients are shown to drive the residual stress.

4

First, we examine the turbulence intensity levels of four cases. As is also shown in the right panel of Fig. 2, the volume-integrated turbulence intensities in the steady state are actually on the same level for the four cases, roughly independent of the current. At the same time, the turbulence intensity gradient, which can also contribute to driving residual stress with an asymmetric fluctuation spectrum in $k_{\parallel}$ due to turbulence wave radiation induced wave momentum diffusion [12], also does not show significant current dependence that can account for the torque vs I_p scaling observed in our simulations. Hence, this implies that the underlying physics for the current scaling has to do with the symmetry breaking dynamics and the associated nonvanishing spectrally averaged $k_{\parallel}$. As we found previously, the turbulence self-generated zonal flow shear is a key mechanism for the symmetry breaking. Simulations also indicate the existence of other mechanisms beyond $\mathbf{E} \times \mathbf{B}$ shear. These include the magnetic shear, to be discussed below.
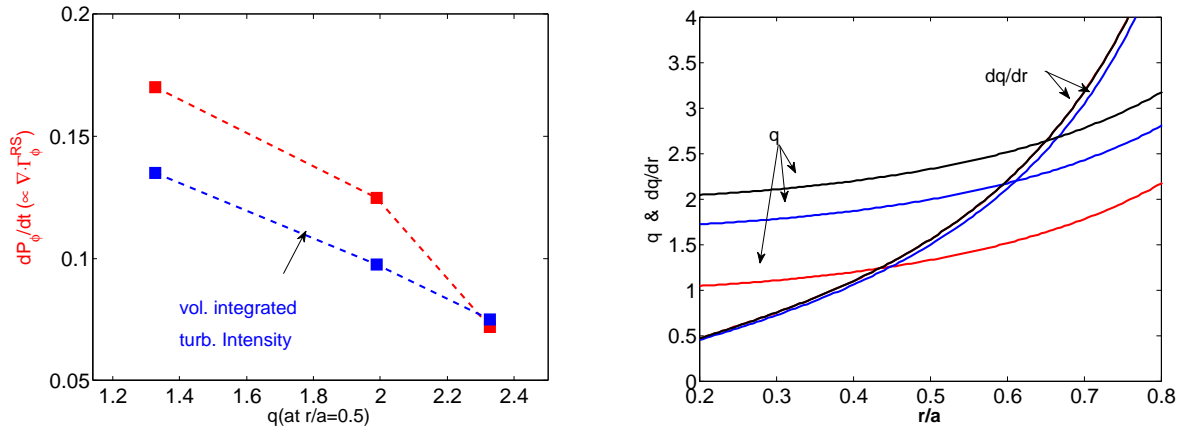

Figure 3: CTEM-driven total intrinsic torque versus q value averaged over the core region (left) and corresponding radial profiles of q and dq/dr for the three equilibria used for these simulations (right).

On the other hand, the corresponding q profile is remarkably boosted in the four equilibria as the plasma current is decreased from 2MA to 0.75MA, as shown in the middle panel of Fig. 2. So is the magnetic shear dq/dr (left panel of Fig. 2). Note that the parameter $\rho_*(\equiv \rho_i/a)$ for the four cases is roughly the same, i.e., $a/\rho_i \sim 170$, which is in the DIII-D range. This observation is highly suggestive that the current scaling of intrinsic torque and rotation may have connections with the change in the magnetic shear and/or the value of q.

To identify the effects of the safety factor and the magnetic shear separately, further computational experiments are performed. First, we examine the effect of the q value. To this end, three MHD equilibria are created, which hold the profile of magnetic shear (and plasma pressure) fixed while boosting the q profile, as shown in the lower panel of Fig. 3. As illustrated in the upper panel of Fig. 3, the CTEM driven intrinsic torque is shown to decrease with the increase of the q value for this scan. The dependence of the volume-integrated turbulence intensity on q value plotted in the same figure indicates that this turbulence intensity dependence appears to be a major cause for the observed intrinsic torque vs q dependence. The key point of this interesting result, however, is that the dependence of the torque on the q value shows the opposite trend to the current scaling obtained in Fig. 2. Therefore, the current scaling is not due to the effect of the q value on the nonlinear residual stress generation.

Now we turn to exploring the effects of the magnetic shear on the intrinsic torque. To this end, three MHD equilibria are created, which hold the radially averaged q value nearly fixed in the central core region where CTEM turbulence is generated, but allow minor variation in the q profile in order to create significant variation in the magnetic shear, as illustrated in the middle and right panels of Fig. 4. At the same time, the plasma pressure is also held fixed. Note that a normal (positive) magnetic shear is presented in these equilibria.
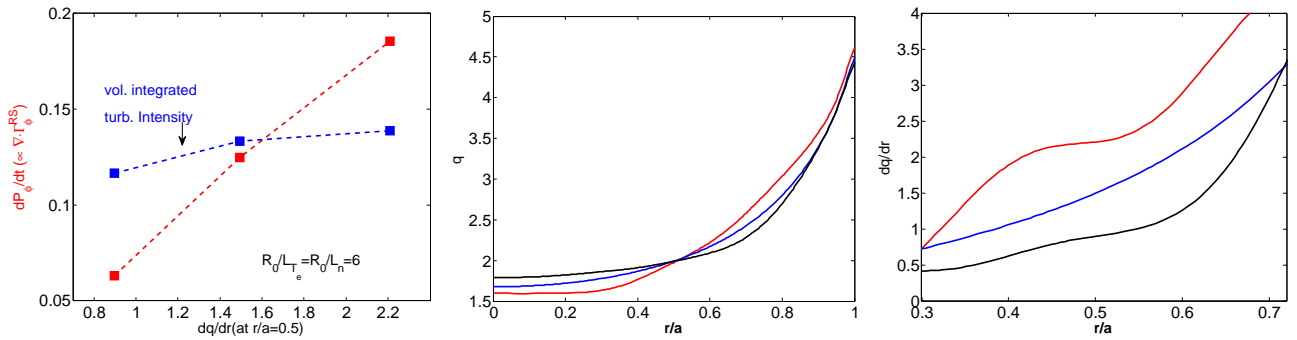
Figure 4: CTEM-driven total intrinsic torque versus magnetic shear averaged over the central core region (left), and corresponding radial profiles of q (middle) and dq/dr (right) of the three equilibria used for these simulations.

The result of this simulation scan is presented in the left panel of Fig. 4, which shows that the volume-integrated intrinsic torque increases nearly linearly with the magnetic shear. On the other hand, the volume-integrated fluctuation intensity exhibits a much weaker dependence on the magnetic shear, which indicates that the observed intrinsic torque vs the magnetic shear scaling mostly results from the effect of the $k_\parallel$ symmetry breaking physics. Specifically, the enhancement of CTEM driven intrinsic torque with magnetic shear is caused by the enhanced $k_\parallel$ symmetry breaking due to stronger magnetic shear. The key point of this result is that the dependence of the intrinsic torque on dq/dr indeed produces the right trend which is consistent with the current scaling obtained in Fig. 2. Therefore, given the distinct effects of varying the q value and the magnetic shear on intrinsic torque generation, it is concluded that the current scaling results

Figure 5: Total intrinsic torque versus external magnetic field B_{vac} in CTEM turbulence.

from the effect of magnetic shear on the turbulence spectrum, namely, the magnetic shear induced $k_\parallel$ symmetry breaking, which is enhanced with increased magnetic shear. We should point out that the effect of magnetic shear on the nonlinear residual generation and the associated key role of it behind the current scaling revealed by these gyrokinetic simulations should be tested and validated by experiments. To a certain extent, this can be done by revisiting the experimental data base from which the current scaling was revealed.

For current scan studies, another scenario often adopted in experiments is to hold the q profile and the pressure profile fixed, while varying the current. In this case, the vacuum magnetic field has to change correspondingly, according to $B_{\text{vac}} \propto I_p$. Our nonlinear CTEM simulations have been also carried out to explore the current dependence of intrinsic rotation in this scenario. We used the same simulation parameters as in Fig. 4, except for the MHD equilibria. Simulation results are presented in Fig. 5. In this case, the CTEM driven intrinsic torque is found to increase close to linearly with the vacuum field. It is important to notice that in this scan scenario, the parameter ρ_* for the three cases varies significantly, from $a/\rho_i \sim 130$ for $B_{\text{vac}} = 1.5$ Tesla to $a/\rho_i \sim 230$ for $B_{\text{vac}} = 2.5$ Tesla, which is an important factor impacting turbulence transport. Thus, the variation in ρ_* should be token into account when we look into the results in Fig. 5 in connection with the experimental scaling. Nevertheless, this current scan scenario is considered to be less relevant to the current scaling obtained in experiments.
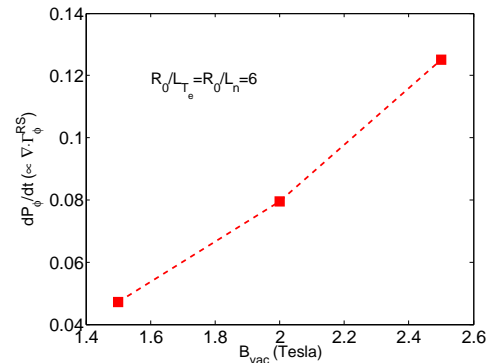
6

IV. Meso-scale phenomena in CTEM turbulence – flow, particle and heat pinch and large scale structure formation

A few highly remarkable, interesting features observed in our CTEM simulations are discussed in this section.
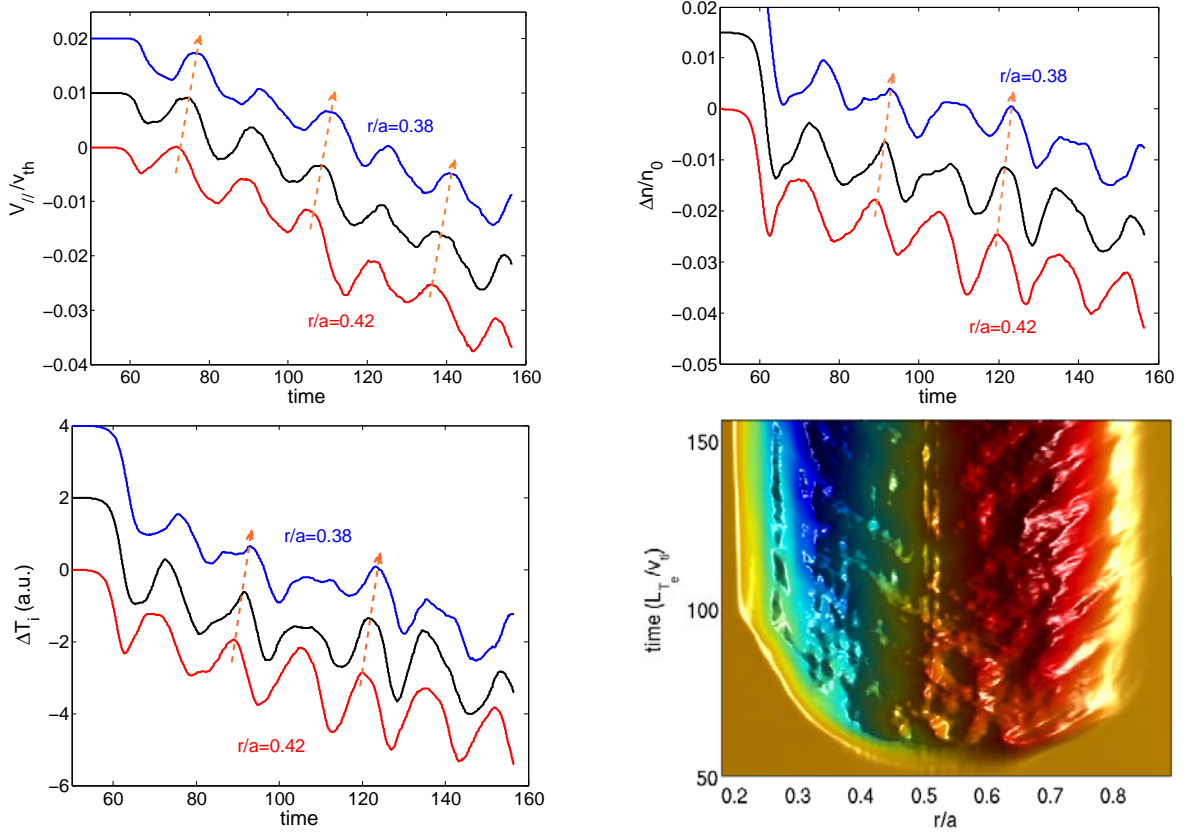

Figure 6: Time history of parallel flow (upper-left), density (upper-right) and ion temperature ΔT_i (lower-left) at three radial locations, and spatio-temporal evolution of electron temperature ΔT_e (lower-right), illustrating generic pinch phenomenon in CTEM turbulence.

First, nonlinear GTS simulations have found that meso-scale phenomena and associated nonlocal transport are highly pronounced in the TEM turbulence regime, probably because of strong coherent wave-particle interaction at magnetic precession resonances of trapped electrons. Remarkably, the parallel (and toroidal) flow exhibits coherent temporal burstings and radial propagation during its generation process, as is clearly seen in the upper-left panel of Fig. 6. Particularly, it is shown that small parallel flow perturbations are generated locally (in the center of the plasma in the simulation case) by the turbulence, and then propagate radially. The measured propagation velocity is $\sim 7 \times 10^{-3} c_s$ with c_s the sound speed. This "flow pinch" phenomenon observed in the simulations appears to phenomenologically reproduce a well-known experimental result in JT-60U where perturbed flows created by modulated beams were demonstrated to penetrate radially from the peripheral region of the plasma into the core [3]. Thus, it is highly illuminating. Furthermore, radial pinches appear to be a very robust and generic feature in CTEM turbulence, and are found to emerge in all transport channels, including particle, electron heat and ion heat. These are illustrated in Fig. 6. One highly remarkable fact found is that the radial pinches in different transport channels emerge "in phase". We point out that the density pinch and heat pinch carried by electron turbulence as suggested by our nonlinear CTEM simulations can be tested by designing similar perturbative experiments to ones with modulated flows.

Finally, as a remarkable meso-scale phenomena, ∇T_e-driven CTEM turbulence in specific, experimentally relevant parameter regimes is found to generate large fluctuation structures with toroidal mode number $n \lesssim 10$ via dramatic inverse energy cascades, as shown in Fig. 7. This phenomenon may have a natural connection to the generation of blobs widely observed in the tokamak edge region.
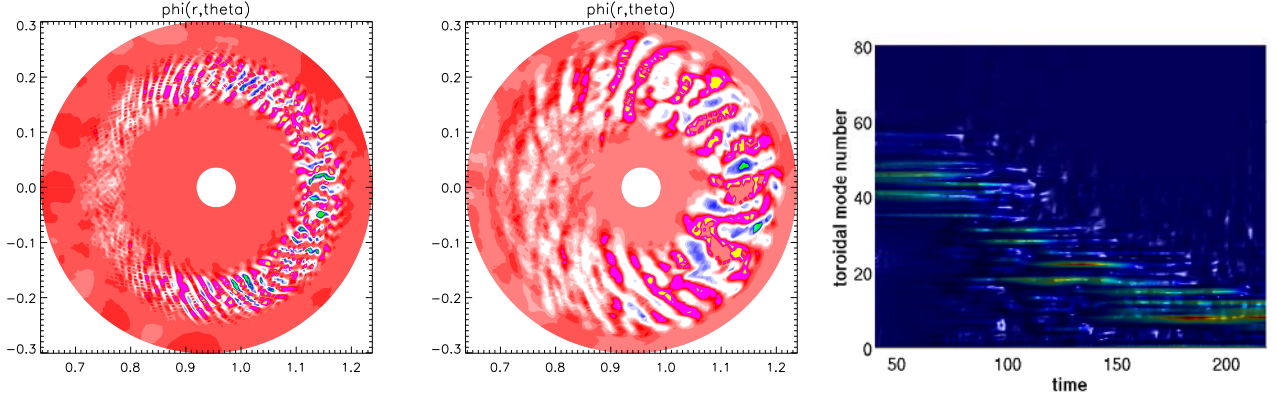

Figure 7: Contour plots of density fluctuations on a poloidal plane at $t = 60$ (left) and $t = 160$ (middle), and time evolution of toroidal spectrum $|\delta n_n|^2$ (right) in ∇T_e-driven CTEM turbulence, showing the generation of low-n, blob-like, large fluctuation structures.

References

[1] J. E. Rice *et al.*, Nucl. Fusion **44**, 379 (2004).

[2] J. E. Rice *et al.*, Nucl. Fusion **47**, 1618 (2007).

[3] M. Yoshida *et al.*, Phys. Rev. Lett. **100**, 105002 (2008).

[4] K. Ida *et al.*, Nucl. Fusion **50**, 064007 (2010).

[5] W. X. Wang *et al.*, Phys. Plasmas **13**, 092505 (2006).

[6] W. X. Wang *et al.*, Phys. Plasmas **17**, 072511 (2010).

[7] S. D. Scott *et al.*, Phys. Rev. Lett. **64**, 531 (1990).

[8] P. H. Diamond *et al.*, Phys. Plasmas **15**, 012303 (2008).

[9] W. X. Wang *et al.*, Phys. Rev. Lett. **102**, 035005 (2009).

[10] R. Dominguez and G. M. Staebler, Phys. Fluids, B **5**, 3876 (1993).

[11] O. D. Gurcan *et al.*, Phys. Plasmas **14**, 042306 (2007).

[12] P. H. Diamond *et al.*, Nucl. Fusion **49**, 045002 (2009).